16th World Conference on Earthquake Engineering, 16WCEE 2017

Santiago Chile, January 9th to 13th 2017

Paper N° 3670

Registration Code: S-S1464596461

IDA-BASED RESEARCH ON DISPLACEMENT DUCTILITY AND SEISMIC FRAGILITY OF CONTINUOUS GIRDER BRIDGE IN HIGH-SPEED RAIL

Y. Ni(1), G. Lu(2), X. Yang(3), H. Jiang(4) and B. Zhao(5)

(1) PhD, Associate Professor, School of Civil Engineering, Beijing Jiaotong University, yjni@bjtu.edu.cn

(2) Graduate Student, School of Civil Engineering, Beijing Jiaotong University, 1192753084@qq.com

(3) Graduate Student, School of Civil Engineering, Beijing Jiaotong University, 761209436@qq.com

(4) PhD, Associate Professor, School of Civil Engineering, Beijing Jiaotong University, jianghui@bjtu.edu.cn

(5) PhD, Professor, School of Civil Engineering, Beijing Jiaotong University, bmzhao@bjtu.edu.cn

Abstract

Comparatively huge dimensions of the cross-sections of the girder and pier of the bridges in high-speed rail were applied to cater for demand of the railway smoothness and the passengers comfort. Whether the seismic performance of the girder bridges satisfied the target performance of the three level seismic fortification targets coded in the existing *Code for seismic design of railway engineering (GB50111-2006) (2009 version)*, is an extensively concerned question in the engineering field. A typical three span continuous girder bridge as the case bridge, the different finite element models are constructed for the different pier height and bridge arrangements using Opensees software. The incremental dynamic analysis (IDA) method is used to analyze the longitudinal seismic performance of the bridges above mentioned. It is shown that pier height and bridge arrangements have little influence on the displacement ductility coefficients for the moderate damage limit state, ranging as 2.31 to 2.38, meanwhile for the severe damage limit state, the displacement ductility coefficients can be close to 7.84 ~ 8.25, those are significantly greater than the allowable ductility coefficient of 4.8. Within the pier height range of 10 to 20m, the height of the fixed pier is the fundamental factor which affects the seismic performance of the pier; while the bridge arrangements with different pier heights are the slight factor. During the design reference period, the bridge piers in high-speed rail will be substantially slight and moderate damaged with high probability; the severe damage probability is about 30%; and the occurring probability of the complete damage (collapse) is as small as being neglected.

Keywords: High-speed rail; Continuous girder bridge; Incremental dynamics analysis; Displacement ductility; Seismic fragility

1. Introduction

The *Code for seismic design of railway engineering* (GB50111-2006) [1] has been modified as 2009 version [2] after the 2008 Wenchuan earthquake in China. The seismic design of the bridges in high-speed rail has been included as Type B and Type C bridges in the code. The important coefficient for the frequently occurred earthquake has been increased from 1.4 to 1.5 for the Type A and Type B bridges.

A series of achievements have been obtained in the ductility design of structures in recent years. Damage indices respecting on the bridge piers with different heights from 6m to 15m were calculated by X. Zhu and H. Jiang [3]. It was shown that the damage index and the displacement ductility for the specific damage state increased with the pier heights. H. Liu [4] calculated the values of the displacement ductility of the railway bridge piers considering the difference of the low reinforcing ratios. The results showed that the longitudinal reinforcing ratio has the great effect on the displacement ductility. Based on the scaled model tests with the column cross-section as 0.9m×0.9m, the ductile capacities of ordinary reinforced concrete columns, core steel reinforced concrete columns and steel pipe columns have been researched by S. Dong. [5]. Considering the parameter variation such as the reinforcing ratios, volume stirrup ratio and the axial compression ratio, L. Yang and J. Xiao [6] analyzed the influential effects respecting to a continuous girder bridge (100m+160m+100m) in a highway. Y. Zhuo and F. Wang [7] made a research on the displacement ductility of a continuous girder bridge (25m+30m+25m) with the pier cross-section as 1.6m×2.2m in a high-speed rail. It was shown that the displacement ductility under the rare occurred earthquake would reach to 3.02.

The fragility curve is generally used to evaluate the seismic performance of the structures. Based on the damage index analysis of the capability-demand ratio, the fragility curves of the bridge pier and the seating of a simply supported steel girder bridge (with the span arrangement (30m+36m+30m), the pier diameter 0.9m, the longitudinal reinforcing ratio 0.103% and the volume stirrup ratio 0.28%) were constructed respectively by Y. Pan [8]. Applying the joint probability considering the earthquake intensity and the epicentral distance, the curved surface was constructed to evaluate the seismic performance of the bridge. C. Zhou and J. Chen [9] researched the seismic vulnerability of a hollow pier in a high-speed rail (height of 99m) based on the curvature analysis of the key section of the pier. Using the damage model proposed by Hwang, P. Yang and G. Yang [10] researched the fragility of the piers with the different pier heights from 3m to 40m and the cross-section from 2.1m×3.6m to 5.0m×6.8m. Applying the incremental dynamic analysis (IDA) method, X. Han and B. Zhu [11] obtained the fragility curves for four damage states of a continuous girder bridge (32m+48m+32m) in high-speed rail based on the damage indices of section curvature. They concluded that the damage probabilities for the slight damage and moderate damage state were determined by the damage level of the piers.

İn order to satisfy the comfort of the high-speed rail, comparativly big size of the bridge section was applied in the continuous girder bridge. While, the low longitudinal reinforcing ratio and volume stirrup ratio are adopted those are different with the railway and highway bridges. Y. Cui et al [12] made a statistical analysis on the piers cross-section, longitudinal reinforcing ratio and volume stirrup ratio those from 9 continuous girder bridges with different span arrangements. İt was shown that the pier section area was between 32 m^2 and 62m^2, the longitudinal reinforcing ratio was between 0.5% and 1.14%, the volume stirrup ratio was between 0.26% and 0.63%. Generally speaking, the longitudinal reinforcing ratio of the bridge pier in high-speed rail is lower than those bridges in railway and highway engineering. Whether the seismic performance of the continuous girder bridges in high-speed rail satisfied the target performance respecting to the three-level fortification earthquakes is extensively highlighted in the field.

In this paper, using IDA method, the displacement ductility and vulnerability of the continuous girder bridge in high-speed rail are analyzed considering the different pier heights and pier arrangements.

2. Parameter Selection and Termination Condition in IDA Method

2.1 Parameter selection of earthquake intensity measure and demand measure

Incremental dynamic analysis is a familiar method to evaluate the seismic performance. The earthquake intensity measure (IM) and the engineering demand measure (DM) should be selected.

Generally the peak ground acceleration (PGA), spectral acceleration S_a and peak ground velocity (PGV) are used to scale the earthquake intensity. The diversity of the seismic response results from the time history analysis based on S_a is much smaller than those from PGA for the regular bridge, which the structure response is controlled by the first mode. Considering the participation of the multiple modes in the response and the scaling index in the seismic code in China, PGA is selected as the IM parameter. The horizontal displacement and the displacement ductility are selected as the DM parameters.

2.2 Definition of the termination condition in IDA method

IM criterion and DM criterion are generally used to define the termination condition [13]. According to the IM criterion, termination condition is defined when the ration of the connecting slope of DM_i and DM_{i+1} in the IDA curve and the elastic slope are lower than 0.2. This method is simple and rough that may reach an irrational limit state. Relying on the actual structural response, the termination condition is defined when the DM value is greater than the collapse controlled threshold value C_{DM} according to the DM criterion. Considering the target performance respecting to the three levels in Chinese seismic code, DM criterion is selected to define the damage state and the target performance. Referring the *Code for seismic design of railway engineering* (GB50111-2006, 2009 version) and *Code for seismic design of Building* (GB50010-2010), the damage states, target performance and the control parameters are listed in Table 1.

Table 1 - The damage states and performance objectives

Damage state	Target performance	Damage characteristics	Control parameters in calculation	
			ε_c	ε_s
Without damage	—	Perfect or locally cracked of concrete	ε_{crack}	—
Slight damage	Bridge is without damage under frequently occurred earthquake	Extensively minor cracks and without spalling of the protective concrete cover	0.004	ε_y
Moderate damage	Bridge is repairable under design earthquake	Post yielding of the reinforcing bars and spalling of the protective concrete cover	0.01	0.01
Severe damage	Bridge is severe damaged without collapse	Largely spalling of the protective concrete cover and the strain of the reinforcing bar is greater than the design value without failure.	ε_{cu}	0.05
Collapse	—	The first rupture of the stirrup bar and the core concrete is crushed.	—	—

Notation: ε_c is the strain of the core concrete; ε_s is the strain of the longitudinal reinforcing bar; These two parameters are respecting to the upper limit of the damage state.

3. Calculation Model of the Case Bridge

3.1 Introduction of case bridge

The case bridge (40m+64m+40m) with pile foundation is selected from the high-speed rail from Beijing to Shanghai. The main beam is made of C50 concrete with varied cross section. The pier is designed as round-end shape with C35 concrete. The pier height is allocated as 21m, 21m, 20m and 11.5m in sequence. The longitudinal reinforcing ratio and the stirrup ratio are listed in Table 2. The site of the case bridge is type III. The designed fortification PGA is 0.2g with 475 years return period.

Table 2 - Reinforcement of the cross sections of pier bottoms

Piers number	1#、4#	2#	3#
Area (m^2)	24.82	32.35	32.35
Longitudinal reinforcing ratio ρ_l(%)	0.483(ϕ25)	0.548(ϕ28)	0.489(ϕ25)
Volume stirrup ratio ρ_w(%)	0.553(ϕ12)	0.491(ϕ12)	0.491(ϕ12)

The finite element model of the case bridge is constructed using Opensees software as Figure 1.

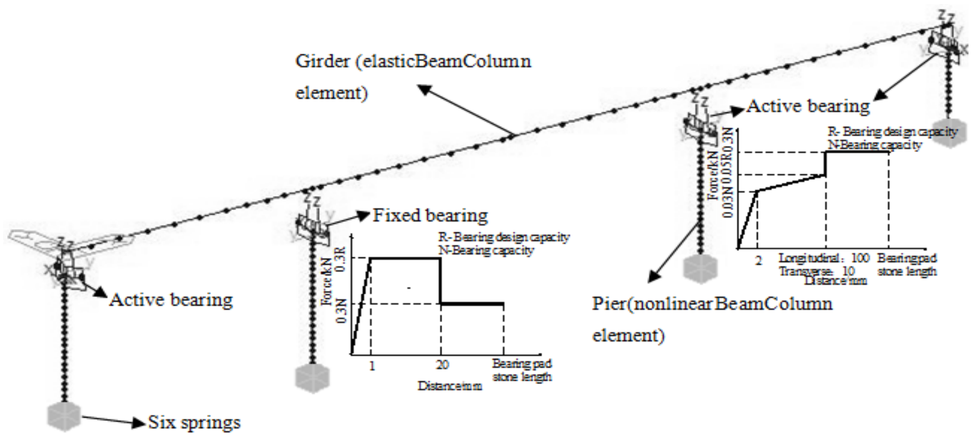

Fig. 1 - Finite element model of the bridge based on Opensees

The seating behavior is defined according to the model proposed by Y. Cui et al. [12]. Six springs are allocated under the platform bottom to consider the pile-soil interaction. Considering the variation of the piers heights and piers allocation, a series of calculating models are constructed as listing in Table 3. It is seen from Table 3 that the first period is controlled by the pier height, while the second period is greatly influenced by the arrangement of the pier height.

Table 3 - Vibration characteristics of different bridge models

Bridge type	Arrangement of pier height (m)	First period (s)	Vibration characteristics	Second period (s)	Vibration characteristics
Actual bridge	21-21-20-11.5	1.00	Longitudinal translation	0.77	Transverse translation with rotation around longitudinal direction
Equal pier height	20-20-20-20	1.16	Longitudinal translation	0.78	Transverse translation with rotation around longitudinal direction
	15-15-15-15	0.90		0.68	
	10-10-10-10	0.70		0.60	
Varied pier height	10-20-10-20	1.16	Longitudinal translation	0.69	Transverse translation with rotation around longitudinal direction
	10-20-20-10	1.16		0.76	
	20-10-10-20	0.70		0.63	Transverse translation with rotation around longitudinal or vertical direction
	20-10-20-10	0.70		0.69	

3.2 Simulation of plastic hinge and analysis on moment-curvature of control section

3.2.1 Model of plastic hinge

The plastic hinge is simulated by fiber hinge at the bottom of the pier. According to the longitudinal reinforcing ratio and stirrup ratio of the pier, adopting the confined and unconfined concrete model proposed by J.B. Mander et al.(1988) [14], the mechanics indices are calculated and listed in Table 4. The Menegotto-Pinto model is used to simulate the behavior of reinforcing bar. Its yielding strength f_y and initial elastic modulus E are 335MPa and 200×10^3MPa, respectively. The ratio of the post-yielding stiffness and the initial stiffness is 0.01.

Table 4 - Index of confined concrete

Pier number	Cubic compression strength (MPa)	Prismatic compression strength (MPa)	Compression strength of confined concrete (MPa)	Peak compression strain of confined concrete	Ultimate compression strain of confined concrete
1#、4#	35	24.5	28.86	0.003779	0.01478
2#、3#	35	24.5	28.29	0.003545	0.01377

The empirical formula as Eq. (1) proposed by Eurocode 8 [15] is used to calculate the length of plastic hinge of the pier.

$$L_p = 0.1L + 0.015 f_y d_b \tag{1}$$

where, L is pier height in m; f_y is the yielding strength of the reinforcing bar in MPa; d_b is the diameter of the reinforcing bar in m.

3.2.2 Analysis on the moment-curvature of pier section

Based on the dimension and reinforcing ratio of pier section, the moment-curvature relations for the bottom section of the pier with different pier heights are analyzed using Xtract software according to the *Seismic Retrofitting Manual for Highway Bridges* (1995) [16]. The equivalent yielding displacement ductility ratio and the maximum displacement ductility ratio under monotonic loading are calculated and listed in Table 5.

Table 5 - Results from the moment-curvature analysis

L	P	L_p	M_{ye}	φ_{ye}	M_u	φ_u	μ_{ye}	$\mu_{\max}$
10	36100	1.14	162.4	0.7851	204.0	13.65	1.15	8.89
15	40100	1.64	169.8	0.7860	210.5	13.70	1.14	8.52
20	44100	2.14	177.3	0.7877	216.8	13.77	1.13	8.32
21	45000	2.24	179.0	0.7885	218.3	13.82	1.13	8.31

Notation: in Table 5, L and L_p are pier height and lenth of plastic hinge in m, respectively; P is the axial compression in kN; M_{ye} and M_u are equivalent yielding moment and ultimate moment in 10^3kNm under monotonic loading, respectively; φ_{ye} and φ_u are equivalent yielding curvature and ultimate curvature in 10^{-3}m^{-1} under monotonic loading, respectively; μ_{ye} and $\mu_{\max}$ are equivalent yielding displacement ductility and maximum displacement ductility ratio, respectively.

3.2.3 Determination of the failure mode of the pier

The failure mode of bridge pier can be predertermined according to Caltrans (Version 1.7, 2013) [17] as Eq. (2).

$$\phi V_n \geq V_0 \tag{2}$$

where V_n is nominal shear capacity; ϕ is the reduction coefficient, designated as 0.85; V_0 is shear force for the overstrength state. V_n can be calculated according to Eq. (3) proposed by Priestley et al [18].

$$V_n = V_c + V_s + V_p \tag{3}$$

where V_c, V_s and V_p are shear capacity provided by the concrete, stirrup bar and axial compression force, respectively.

V_0 can be calculated according to Eq. (4) coded in Caltrans (Version 1.7, 2013) [17].

$$V_0 = \frac{M_0}{L} = \frac{\lambda_0 M_R}{L} \tag{4}$$

where M_R is the nominal bending moment, λ_0 is the overstrength coefficient, designated as 1.2.

The calculation results of the failure mode of the different bridge piers are shown in Fig.2. It can be seen from Fig.2 that shearing force of all piers before the failure state are far lower than those nominal shear capacity. The failure mode of the bridge piers can be predetermined as bending failure mode.

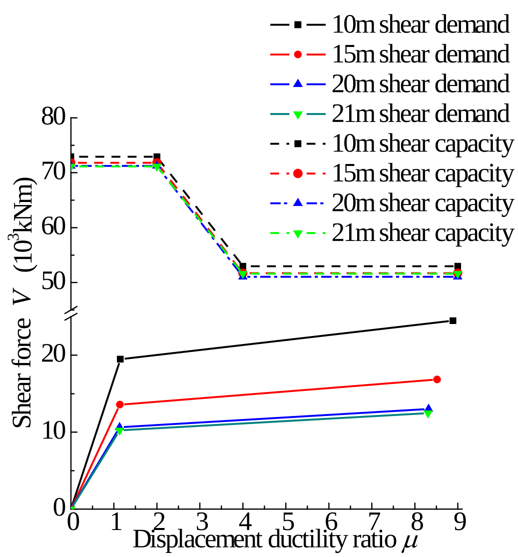

Fig.2 - The displacement ductility ratio of piers with different heights as failing

4. Selection of Earthquake Ground Motion

Considering the factors such as site type, the predominant period of the earthquake wave, the fundamental period of the case bridge, earthquake intensity and its PGA , and the epicentral distance of the earthquake record, altogether 15 (listed in Table 6) records are selected from the database provided by PEER website.

Table 6 - Earthquake records information

Number	Earthquake records	Moment magnitude	Fault distance(km)	Time	Predominant period(s)	PGA (g)
1	LOMAP/HVR090	6.9	31.6	1989	0.58	0.103
2	LOMAP/A2E000	6.9	57.4	1989	0.48	0.171
3	LOMAP/SJW250	6.9	32.6	1989	0.50	0.112
4	LOMAP/NAS180	6.9	75.2	1989	0.63	0.268
5	LANDERS/IND090	7.3	55.7	1992	0.50	0.109
6	LOMAP/SLAC	6.9	30.6	1989	0.49	0.277

Number	Earthquake records	Moment magnitude	Fault distance(km)	Time	Predominant period(s)	PGA (g)
7	CAPE MENDOCINO	7.0	40.3	1992	0.67	0.154
8	IMPVALL/H-CC4135	6.5	49.3	1979	0.56	0.128
9	IMPVALL/H-CC4045	6.5	49.3	1979	0.44	0.115
10	KERN/TAF021	7.4	41.0	1952	0.36	0.156
11	CAPEMEND/EUR090	7.1	44.6	1992	0.52	0.178
12	BIG BEAR-01	6.5	33.6	1992	0.52	0.111
13	LOMAP/DUMB357	6.9	35.5	1989	0.75	0.127
14	IWATE /JAPAN	6.9	31.9	2008	0.53	0.167
15	DARFIELD/ NEW ZEALAND	7.0	30.5	2010	0.50	0.360

The dynamic amplification coefficients of 15 earthquake waves are calculated and demonstrated in Fig.3. It can be seen from Fig.3 that the mean value of results from selected 15 records are close to the design spectrum coded in *Code for seismic design of railway engineering* (GB50111-2006, 2009 version) within the period domain from 0.5s to 3s, namely that the selection of the 15 records is proper.

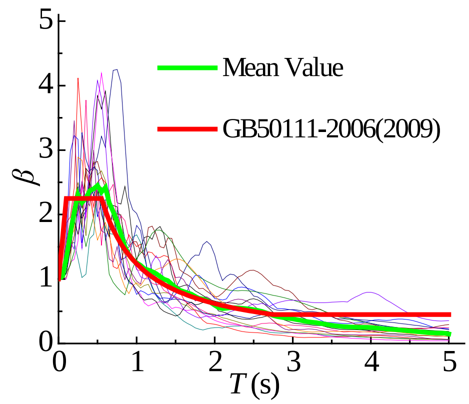

Fig.3 - Dynamic amplification factor spectrum

5. Displacement Ductility of Bridge Models

In order to develop the influence of pier height arragement on the displacement ductility, bridge models with different pier heights and pier arrangements are constructed. Defining PGA as the IM parameter and displacement of the pier top Δ as the DM parameter, considering the control parameters listed in Table 1 for different damage state, the IDA curves for the bridge models are obtained through the incremental dynamic analysis and shown in Fig.4.

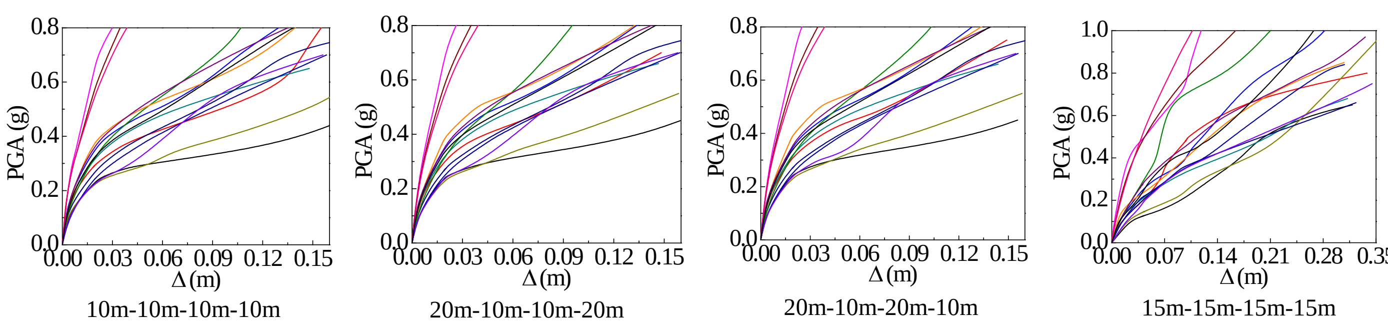

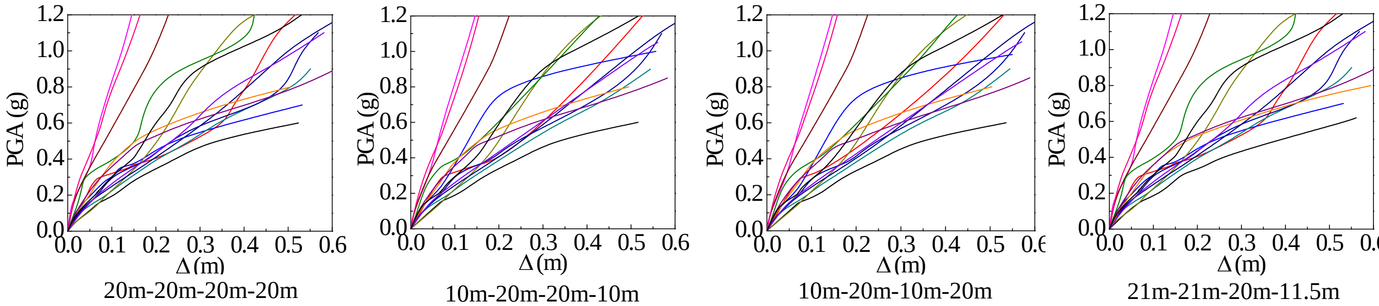

Fig.4 - IDA curves for the full bridge models with different pier arrangement

It can be known based on the IDA procedure that the top displacement of the pier with fixing seating are consistent with the peak curvature of the control section, similarly the material damage are consistent with the deformation. The damage states are controlled by the strain level of the longitudinal reinforcing bar, rather than the compression strain of the core concrete. For example, in case of the actual bridge, when the tensile strain of the reinforcing bar of the pier with fixing seating reaches to 0.05, the compression strain of the core concrete only reaches 0.005, which is far lower than its ultimate compression strain, namely that the core concrete cannot reach the crush state.

It can be seen from Fig.4 that the PGA values respecting to the collapse controlled state of the short piers (10m) are significantly lower than those of high piers, namely the ductile capacity of high pier is superior to the short pier. Provided the same height of the pier with fixing seating, the yielding displacement and the ultimate displacement of the bridge models are similar.

The yielding displacement, mean values of the ultimate displacements and the displacement ductility coefficients respecting on the moderate damage state and severe damage state results from the IDA using 15 earthquake records are listed in Table 7.

Table 7 - The summary of the full bridge models along the longitudinal direction according to the IDA results

Bridge type	Pier height (m)	Yielding displacement (m)	Maximum displacement of moderate damage state (m)	Maximum displacement ductility coefficient of moderate damage state	Ultimate displacement of severe damage state (m)	Ultimate displacement ductility coefficient of severe damage state
Actual bridge	21-21-20-11.5	0.0727	0.1690	2.32	0.5828	8.05
Equal pier height	20-20-20-20	0.0719	0.1675	2.33	0.5771	8.03
	15-15-15-15	0.0409	0.0950	2.33	0.3237	7.92
	10-10-10-10	0.0193	0.0459	2.38	0.1576	8.18
Varied pier height	10-20-10-20	0.0733	0.1689	2.31	0.5742	7.84
	10-20-20-10	0.0725	0.1713	2.37	0.5739	7.93
	20-10-10-20	0.0192	0.0454	2.37	0.1581	8.25
	20-10-20-10	0.0191	0.0445	2.33	0.1574	8.23

Following conclusions can be obtained from Table 7:

(1) The calculated displacement ductility coefficients are between 2.06 and 2.38 for the moderate damage state, which are far lowen than the allowable displacement ductility coefficient 4.8; while for the severe damage state, those coefficients are between 7.84 and 8.25, those are far greater than 4.8.

(2) The influence of the pier height on the displacement ductility coefficient are not obvious.

6. Seismic Vulnerability of Bridge Models

In this paper, the standard deviation of the damage indices are directly regressed by polynomial curves instead of the combination value results from the statistical dispersion coefficient proposed by HAZUS99. The exceedance probabilities of bridge models for different damage state can be calculated by Eq. (5).

$$P_f = P\left[\frac{s_d}{s_c} \geq 1\right] = 1 - \phi\left[\frac{\ln(1) - \lambda}{\sigma}\right] = \phi\left[\frac{\lambda}{\sigma}\right] \tag{5}$$

where P_f is the exceedance probability for the structural response is greater than the threshold value of a specific damage state; s_d is the earthquake demand of structure; s_c is the structure capacity; λ and σ are regressed mean value and standard deviation using polynominial curve, can be calculated according to Eq. (6) and Eq. (7) , respectively.

$$\lambda = a(\ln(\text{PGA}))^2 + b\ln(\text{PGA}) + c \tag{6}$$

$$\sigma = \sqrt{S_r / (n-2)} \tag{7}$$

where a, b and c are regression coefficients, S_r is the sum of squares of residual error respecting to the discrete points to the regressed curve.

6.1 Determination of the damage index

The upper limit value of the damage index for the without damge state is relied on the crack level of the concrete; While the upper limit values for other damage states are controlled by the strain values of the longitudinal bars. The threshold values μ_c, $\mu_y(\equiv 1)$, μ_m and μ_max for the four states such as without damge, slight damage, moderate damage and severe damage, are statistically analyzed in Fig.5 based on altogether 120 bridge samples.

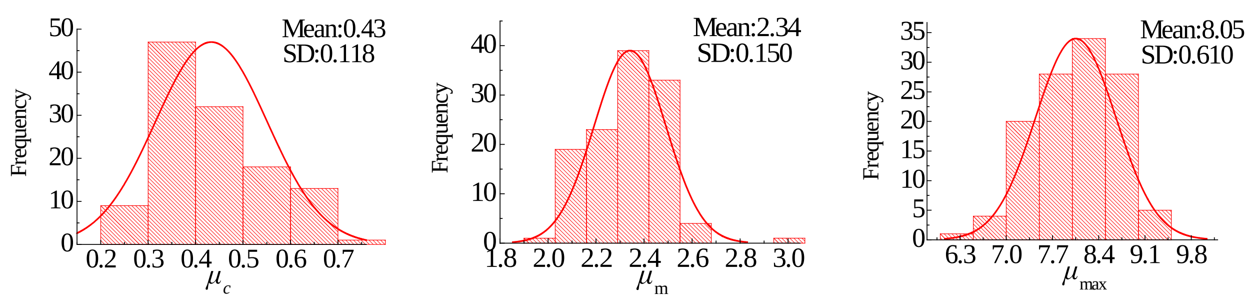

Fig.5 - Statistical results of parameter μ

Notation: in Fig.5, statistical parameter $\mu = \Delta / \Delta_y$, Δ is displacement of pier top under different PGA, and displacement of the pier top Δ_y is corresponding to the initiation of steel bar yielding. So μ_y is identically equal to 1.

It can be seen from Fig.5 that the upper limit values μ_c, μ_m and μ_max for the three states obey the normal distribution. The threshold values for different damage states can be obtained and listed in Table 8.

Table 8 - The threshold values for different damage states

Without damage	Slight damage	Moderate damage	Severe damage
μ_c	μ_y	μ_m	μ_max
0.43	1	2.34	8.05

6.2 IDA curves for the demand-capacity ratio of bridges

Based on the calculating results from IDA, the IDA curves for the demand-capacity ratio (s_d /s_c) and PGA can be obtained. For saving paper, only the curves for the actual bridge are shown in Fig.6.

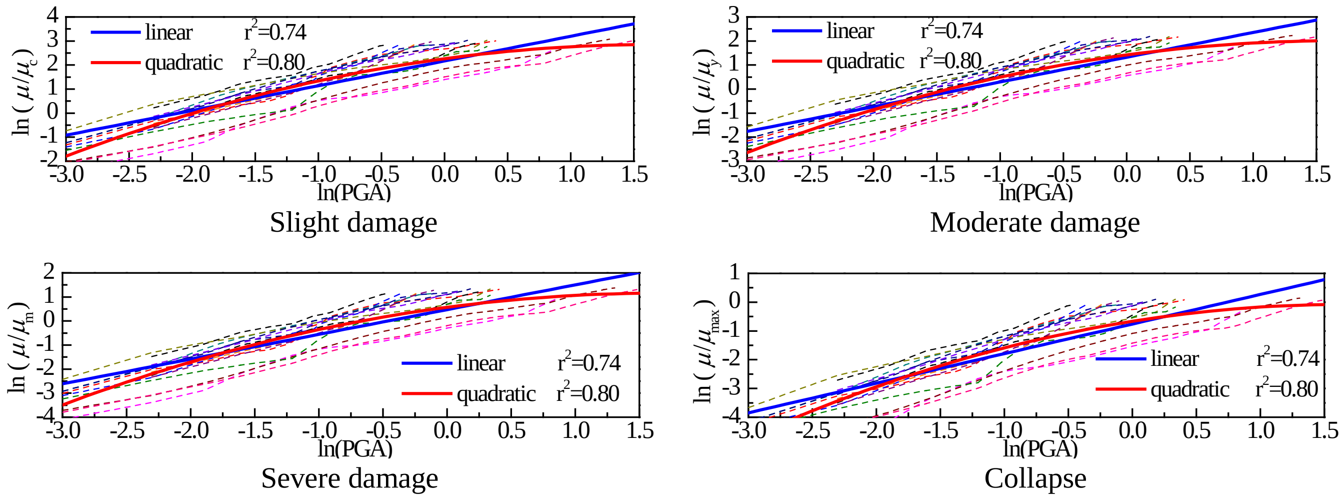

Fig.6 - IDA curves for different damage states at the bottom of pier of span 21m-21m-20m-11.5m

The regression results for bridge models are shown in Table 9. In Fig.6 and Table 9, r^2 means the correlation coefficient to the regressed curve and the calculated curve.

Table 9 - The fitting results of demand-capacity ratio IDA curves for bridge models

Bridge type	Slight damage	Moderate damage	Severe damage	Collapse
21m-21m-20m-11.5m	y=-0.21x^2+0.71x+2.26 r^2=0.80	y=-0.21x^2+0.71x+1.42 r^2=0.80	y=-0.21x^2+0.71x+0.75 r^2=0.80	y=-0.21x^2+0.71x-0.67 r^2=0.80
20m-20m-20m-20m	y=-0.20x^2+0.72x+2.25 r^2=0.80	y=-0.20x^2+0.72x+1.41 r^2=0.80	y=-0.20x^2+0.72x+0.56 r^2=0.80	y=-0.20x^2+0.72x-0.68 r^2=0.80
10m-20m-20m-10m	y=-0.21x^2+0.72x+2.33 r^2=0.78	y=-0.21x^2+0.72x+1.49 r^2=0.78	y=-0.21x^2+0.72x+0.64 r^2=0.78	y=-0.21x^2+0.72x-0.60 r^2=0.78
10m-20m-10m-20m	y=-0.20x^2+0.72x+2.41 r^2=0.81	y=-0.20x^2+0.72x+1.57 r^2=0.81	y=-0.20x^2+0.72x+0.72 r^2=0.81	y=-0.20x^2+0.72x-0.52 r^2=0.81
15m-15m-15m-15m	y=-0.24x^2+0.70x+2.47 r^2=0.75	y=-0.24x^2+0.70x+1.63 r^2=0.75	y=-0.24x^2+0.70x+0.78 r^2=0.75	y=-0.24x^2+0.70x-0.46 r^2=0.75
10m-10m-10m-10m	y=-0.17x^2+1.18x+2.52 r^2=0.82	y=-0.17x^2+1.18x+1.68 r^2=0.82	y=-0.17x^2+1.18x+0.83 r^2=0.82	y=-0.17x^2+1.18x-0.41 r^2=0.82
20m-10m-10m-20m	y=-0.36x^2+0.83x+2.51 r^2=0.79	y=-0.36x^2+0.83x+1.66 r^2=0.79	y=-0.36x^2+0.83x+0.81 r^2=0.79	y=-0.36x^2+0.83x-0.42 r^2=0.79
20m-10m-20m-10m	y=-0.35x^2+0.86x+2.50 r^2=0.79	y=-0.35x^2+0.86x+1.66 r^2=0.79	y=-0.35x^2+0.86x+0.81 r^2=0.79	y=-0.35x^2+0.86x-0.43 r^2=0.79

6.3 Fragility analysis of the bridge models

Based on the regressed equation listed in Table 9, the probability for different damage states respecting to PGA values 0.07g, 0.2g, 0.38g and 0.64g [19] (corresponding to the different return period as 50years, 475years, 2450 years and 10000 years, respectively) can be achieved. The damage probabiltiy values respecting to the different PGA values are listed in Table 10.

Table 10 - The damage probability of models along the longitudinal direction by IDA

Bridge type	PGA=0.07g		PGA=0.2g		PGA=0.38g		PGA=0.64g	
	SLD	MD	MD	SED	SED	C	SED	C
21m-21m-20m-11.5m	1.7%	0.01%	30.3%	1.8%	27.7%	0.19%	65.3%	2.8%
20m-20m-20m-20m	2.1%	0.01%	30.4%	1.8%	26.8%	0.17%	65.4%	2.5%
10m-20m-20m-10m	1.7%	0.01%	33.6%	1.7%	30.6%	0.14%	71.0%	2.7%
10m-20m-10m-20m	0.6%	0	39.9%	1.6%	35.6%	0.10%	78.6%	2.6%
15m-15m-15m-15m	1.8%	0.01%	41.4%	3.0%	40.8%	0.39%	79.6%	5.5%
10m-10m-10m-10m	0.2%	0	14.8%	0.8%	22.7%	0.32%	66.7%	6.1%
20m-10m-10m-20m	0.01%	0	14.9%	0.6%	28.8%	0.38%	73.7%	7.0%
20m-10m-20m-10m	0	0	13.4%	0.5%	26.9%	0.26%	73.5%	6.1%

In Table10, SLD, MD, SED and C mean the slight damage, moderate damage, severe damage and collapse, respectively.

It can be seen from Table 10 that the continuous girder bridge in high-speed rail designed according to the existing code can satisfy the target performance for the three earthquake levels.

The seismic fragility curves for different pier heights and pier arrangemens can be achieved according to the correlation equations corresponding to the different damage states listed in Table 9. For saving paper, only the results corresponding the different pier heights with fixing seating and the different pier arrangements with 20m height of the pier with fixing seating are shown in Fig.7.

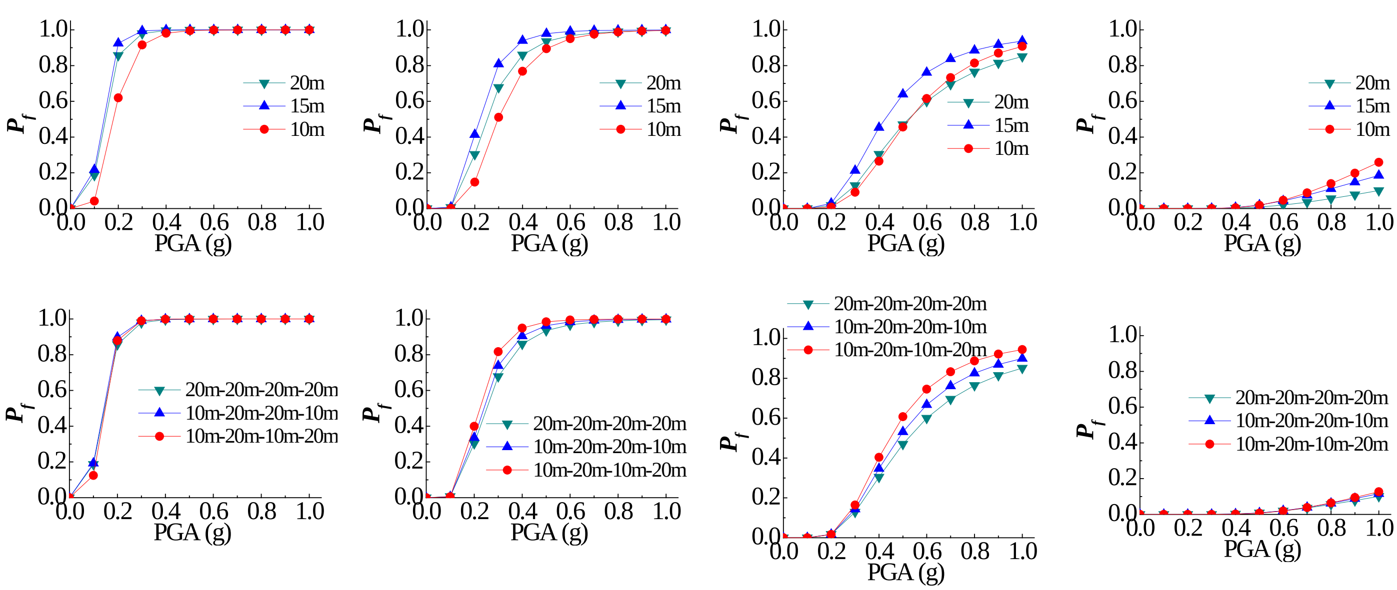

Slight damage　Moderate damage　Severe damage　Collapse

Fig.7 - The fragility curves for the bridges along longitudinal direction

It can be seen from Fig.7 that the pier height has a certain influence, but the different pier arrangement has slightly influence on the damage probability.

7. Conclusion

Based on the analysis of the bridge models constructed in this paper, the following conclusions can be drawn:

(1) Displacement ductility

Consider the actual design condition of the case bridge , the damage state of the continous girder bridge are determined by the tensile strain of the longitudinal reinforcing bar for the pier with fixing seating; the confined effect due to the stirrup bars on the core concrete are strong because of the huge pier cross-section adopted in high-speed rail bridges.

The yielding displacement and ultimate displacement are similar, respectively, provided the equal heights of the pier with fixing seating are adopted.

The allowable ductility coefficient 4.8 coded in *Code for seismic design of railway engineering* (GB50111-2006, 2009 version) is not suitable for the severe damage state. The threshold value of the ductility coefficient should be developed in the further research.

(2) Seismic fragility

The ductile capacity of the high pier (20m height) are superior to those of short pier. The height of the pier with fixing seating has a certain effect on the seismic fragility of the continuous girder bridge in high-speed rail,but the different pier arrangement is so slight.

The seismic performance of the continuous girder bridge designed according to the existing code is excellent for the different earthquake levels.

8. Copyrights

9. Acknowledgement

Authors acknowledge the financial support by the National Natural Science Foundation of China (No. U1434210), Major Issue of Development Plan of China Railway Cooperation, China (No. 2013G002-A-3).

10. References

[1] Code for seismic design of railway engineering (GB50111-2006)[S]. Beijing: China Plan Press, 2006.

[2] Code for seismic design of railway engineering (GB50111-2006) (2009 version)[S]. Beijing: China Plan Press, 2009.

[3] Zhu Xi, Jiang Hui. Performance-based seismic design method for RC bridge piers[J]. China Civil Engineering Journal, 2009, 42(4): 85-92.

[4] Liu Hao. Numerical Stimulation of Rare-Reinforced Concrete Railway Bridge Pier's Seismic Behavior[D]. Dissertation for Master Degree of Beijing Jiaotong University, 2010.6.

[5] Dong Sansheng, Zhao Junhai. Seismic Ductility of Concrete Columns with Different Reinforcement Patterns [J]. China Civil Engineering Journal, 2004, 37(6): 47-51.

[6] Yang Liang, Xiao Jie, Wang Wenxin, Yang Libo. Analysis of Seismic Isolation and Ductility for Long-span Continuous Bridges [J]. Journal of Highway and Transportation Research and Development, 2011, 8(28): 73-78.

[7] Zhuo Yi, Wang Fei. Seismic Ductility Design for Intercity Railway Continuous Bridge under Rare Earthquake[J]. Journal of Railway Engineering Society, 2012, 163(4): 66-71.

[8] Y.Pan, A K Agrawal, M. Ghosn Seismic fragility of continuous steel highway bridges in New York State[J]. J.Bridge Eng. 2007, 12(6): 689-699.

[9] Zhou Changdong, Chen Jing, Zeng Xulang, Liu Bin. Evaluation of Seismic Vulnerability of Reinforced Concrete Circular Hollow High-piers [J]. Journal of Railway Engineering Society, 2014, 194(11): 65-71.

[10] Yang Ping, Yang Guojing, Zeng Yongping. Analysis of Seismic Vulnerability and Adaptation of Simply-supported Girder Bridge on Sichuan-Tibet Railway[J]. Journal of Railway Engineering Society, 2015, 207(12): 51-57.

[11] Han Xing, Li Xin, Xiang Baoshan, Cui Shengai, Zhu Bing. Analysis of Seismic Fragility of High Speed Railway Continuous Beam Bridge Based on IDA Method[J]. Journal of Highway and Transportation Research and Development, 2016, 33(2): 54-59.

[12] Cui Yuting. Study on the Seismic Performance of Large-span RC Continuous Girder Bridge of High Speed Railway and Reasonable Reinforcement Level of Piers[D]. Dissertation for Master Degree of Beijing Jiaotong University, 2015.6.

[13] Dimitrios Vamvatsikos, C. Allin Cornell. Incremental dynamic analysis[J]. Earthquake engineering and structural dynamics.2002, 31: 491-514.

[14] Mander J B, Priestley M.J.N., Park R. Theoretical Stress-Strain model for confined concrete[J].ASCE, Journal of structural Engineering, 1988, 114(8): 1804-1826.

[15] N1998-2:2005: E. Eurcode8-Design Provisions for Earthquake Resistance of Structures, Part2: Bridges[S]. Belgium: Committee European De Normalization (CEN), 2005.

[16] Seismic Retrofitting Manual for Highway Bridges (1995)[S]. Publication No.FHWA-RD-94-052, Office of Engineering and Highway Operations R&D, Federal Highway Administration, McLean, VA.

[17] Caltrans, Seismic Design Criteria, Version l.7[S]. CALTRANS, April 2013.

[18] Priestley M.J.N., Verma R., Xiao Y. Seismic shear strength of reinforced concrete columns[J]. Journal of Structural Engineering, 1994, 120(8): 2310-2329.

[19] Seismic Ground Motion Parameters Zonation Map of China (GB18306-2015).